Available online at www.sciencedirect.com
SCIENCE DIRECT
Journal of Chromatography A, 1125 (2006) 76–88
JOURNAL OF CHROMATOGRAPHY A
www.elsevier.com/locate/chroma

Separation and quantitation of water soluble cellular metabolites by hydrophilic interaction chromatography-tandem mass spectrometry

Sunil U. Bajad [a], Wenyun Lu [a], Elizabeth H. Kimball [a], Jie Yuan [a], Celeste Peterson [b], Joshua D. Rabinowitz [a,*]

[a] *Lewis-Sigler Institute for Integrative Genomics and Department of Chemistry, Princeton University, Princeton, NJ 08544, USA*
[b] *Department of Molecular Biology, Princeton University, Princeton, NJ 08544, USA*

Received 13 January 2006; received in revised form 8 May 2006; accepted 10 May 2006
Available online 6 June 2006

Abstract

A key unmet need in metabolomics is the ability to efficiently quantify a large number of known cellular metabolites. Here we present a liquid chromatography (LC)–electrospray ionization tandem mass spectrometry (ESI-MS/MS) method for reliable measurement of 141 metabolites, including components of central carbon, amino acid, and nucleotide metabolism. The selected LC approach, hydrophilic interaction chromatography with an amino column, effectively separates highly water soluble metabolites that fail to retain using standard reversed-phase chromatography. MS/MS detection is achieved by scanning through numerous selected reaction monitoring events on a triple quadrupole instrument. When applied to extracts of *Escherichia coli* grown in [^{12}C]- versus [^{13}C]glucose, the method reveals appropriate ^{12}C- and ^{13}C-peaks for 79 different metabolites.

Keywords: LC–ESI-MS/MS; *Escherichia coli*; Metabolomics; Metabonomics; Hydrophilic interaction chromatography; Bacteria; Metabolite; metabolism; Triple quadrupole; Mass spectrometry

1. Introduction

The ability to quantify numerous mRNA in parallel using DNA microarrays has revolutionized biological science, with important applications ranging from grouping genes into functional pathways to predicting the progression of human diseases [1]. In the wake of the genomics revolution, there has been a drive to bring similarly comprehensive analysis to other aspects of biology, including metabolism [2–4]. Experimental metabolomics, however, suffers from its lack of a microarray equivalent: a highly parallel assay for quantifying known cellular metabolites.

A first challenge in attempting to quantify every component of the metabolome of an organism is the absence of a master template, analogous to the genome, for cellular small molecules. Nevertheless, analysis of the full genomes of unicellular model organisms suggests that current metabolic maps, which include for *Escherichia coli* some 500 different water soluble compounds, likely capture most key metabolic end products and intermediates [5–8]. Thus, a key current need is an assay that can reliably and efficiently measure these known compounds [9]. Such measurement, however, is difficult, especially due to the low abundance of most cellular metabolites, which in total comprise only ∼3% of *E. coli* dry weight [10].

Various approaches have been applied recently in an effort to measure multiple metabolites. These include thin-layer chromatography [11,12], high-performance liquid chromatography (LC) with detection based on absorption or emission of light [13], nuclear magnetic resonance spectroscopy [14–16] and chromatography coupled to mass spectrometry (MS) [17–22]. Among these approaches, chromatography coupled to MS stands out for its potential for high sensitivity and specificity. In addition, MS offers the opportunity to confirm the molecular formulas of the specific compounds being measured and to conduct isotope-ratio-based quantitation of biological samples [23].

Chromatography-MS methods can be grouped according to the type of chromatography and MS performed. While gas chromatography-MS has proven a powerful tool for evaluating numerous low molecular weight metabolites [22], it is not well

* Corresponding author. Tel.: +1 609 258 8985; fax: +1 609 258 3565.
E-mail address: joshr@genomics.princeton.edu (J.D. Rabinowitz).

0021-9673/$ – see front matter © 2006 Elsevier B.V. All rights reserved.
doi:10.1016/j.chroma.2006.05.019

suited to analyzing metabolites with low volatility and thermal stability, such as phosphate-containing compounds. Thus, much current research focuses on LC–MS with electrospray ionization. While straightforward LC–MS provides a useful tool for initial analysis of samples without prior knowledge of the analytes of interest, for quantifying compounds with known fragmentation patterns, selected reaction monitoring (SRM) using a triple quadrupole instrument offers additional sensitivity and specificity [24]. SRM involves selecting for ions of a specified parent molecular weight (*m*/*z* ratio), fragmenting the parent ion at an optimal collision energy for producing a particular daughter ion, and then quantifying the production of ions of the daughter mass. By scanning through multiple SRM events, it is possible to measure numerous compounds in a single LC run with this approach.

To date, major barriers to employing triple quadrupole LC–MS/MS to quantify cellular metabolites included lack of knowledge of the SRM transitions of most metabolites and the absence of good LC methods for metabolite separation. Here, we address both of these deficiencies for 141 metabolites (Table 1), corresponding to ∼25% of the known metabolome of *E. coli*. These 141 compounds were selected based on their stability, importance to core metabolic processes common also to eukaryotic organisms, and the availability of purified standards of the compounds. They include, for example, 19 of the 20 proteogenic amino acids, 29 nucleotides, 10 components of glycolysis and the tricarboxylic acid (TCA) cycle, and nearly every compound involved in *de novo* pyrimidine biosynthesis. Of these 141 compounds, we are able to quantify 69 from *E. coli* extracts, and find significant changes in 39 upon carbon starvation of *E. coli*.

2. Experimental

2.1. Chemicals, reagents, and chromatography columns

HPLC-grade solvents (OmniSolv, EMD Chemical, Gibbstown, NJ, USA) were obtained from VWR International (West Chester, PA, USA); ammonium acetate (99.4%) and formic acid (88%) from Mallinckrodt Chemicals, Phillipsburg, NJ, USA; and ammonium hydroxide solution (29.73%) from Fisher Scientific, Pittsburg, PA, USA. All purified metabolite standards (Table 1 and Table S-1 of the Supplementary Materials) were obtained through Sigma-Aldrich (St. Louis, MO, USA) and are ≥98% pure according to the manufacturer, with the exception of guanosine 5′-diphosphate, 3′-diphosphate, which was the kind gift of Michael Cashel, National Institute of Child Health and Human Development, Bethesda, MD, USA. All media components (see Section 2.7), were obtained from Sigma-Aldrich and are ≥98% pure according to the manufacturer. [^{13}C]Glucose (99%) was obtained from Cambridge Isotope Laboratories (Andover, MA, USA). Internal standards tested were *N*-acetylglutamine (not isotope-labeled) from Sigma-Aldrich and the following isotope-labeled compounds (uniformly ^{13}C > 98%, ^{15}N > 98% unless otherwise indicated): glutamate, threonine, and succinate (1,4-^{13}C) from Cambridge Isotope Laboratories; and alanine, deoxyadenosine, thymidine, UMP, AMP, ATP, and TTP from Medical Isotopes (Pelham, NH, USA). All chromatog-

Table 1
Metabolites investigated

Amino acids
- **Alanine**
- **Arginine**
- **Asparagine**
- **Aspartate**
- *Cysteine*
- **Glutamate**
- **Glutamine**
- **Glycine**
- **Histidine**
- **(Iso)leucine**
- **Lysine**
- **Methionine**
- **Phenylalanine**
- **Proline**
- Serine
- **Threonine**
- **Tryptophan**
- **Tyrosine**
- **Valine**

Amino acid derivatives/precursors
- 3-Phospho-serine
- **Citrulline**
- Cystathionine
- Histidinol
- *Homocysteic acid*
- Homocysteine
- **Homoserine**
- Hydroxyphenylpyruvate
- *N*-α-Acetylornithine
- **Ornithine**
- *p*-Aminobenzoate/anthranilate
- Phenylpyruvate
- *Prephenate*
- *S*-Adenosyl-L-homocysteine
- ***S*-Adenosyl-L-methionine**
- Shikimate
- Taurine

Nucleoside bases
- **Adenine**
- Cytosine
- **Guanine**
- **Hypoxanthine**
- Thymine
- *Uracil*
- Xanthine

Nucleosides
- **Adenosine**
- **Cytidine**
- **Deoxyadenosine**
- Deoxyguanosine
- Deoxyinosine
- Deoxyuridine
- **Guanosine**
- **Inosine**
- **Thymidine**
- **Uridine**
- Xanthosine

Nucleoside monophosphates
- **AMP**
- **CMP**
- **Cyclic-AMP**
- **damp**
- **dCMP**

Table 1 (*Continued*)

dGMP
dTMP
dUMP
GMP
IMP
UMP
Xanthosine-5-P

Nucleoside di/triphosphates
ADP
ATP
CDP
CTP
dATP
dCDP
dCTP
dGDP
dGTP
dUTP
GDP
GTP
IDP
ITP
dTDP
TTP
UDP
UTP

Nucleotide precursors/derivatives
Carbamoyl-L-aspartate
Carbamoyl-P
Dihydroorotate
Guanosine 5′-PP,3′-PP
N-Acetyl-glucosamine-1-P
Orotate
Orotidine-P
PRPP

CoA's
3-Hydroxy-3-methylglutaryl-CoA
Acetoacetyl-CoA
Acetyl-CoA
CoA
Dephospho-CoA
Malonyl-CoA
Propionyl-CoA
Succinyl-CoA

Carbohydrate derivatives/precursors
2-Dehydro-D-gluconate
3-Phosphoglycerate
6-Phospho-D-gluconate
Acetylphosphate
ADP-D-glucose
Allantoate
Allantoin
Deoxyribose-P
D-Glucarate
D-Hexose-P
Dihydroxy-acetone-P
D-Rib(ul)ose-5-P
Erythrose-4-P
Fructose-1,6-bis-P
Gluconate
Glucosamine
Glucosamine-1-P
Glucosamine-6-P
Glycerate
Glycerol-3-P

Table 1 (*Continued*)

Phosphoenolpyruvate
Trehalose
UDP-D-glucose
UDP-D-glucuronate
UDP-*N*-acetyl-D-glucosamine

Vitamins and derivatives
Biotin
Carnitine
Folate
Nicotinamide
Nicotinate
Pantothenate
Pyridoxine
Riboflavin
Thiamine
5-Methyl-THF
7,8-Dihydrofolate
Thiamine-P

Carboxylic acids
Acetoacetate
Citrate
Fumarate
Malate
Oxaloacetate
Succinate
Aconitate
α-Ketoglutarate

Redox-electron-carriers and precursors
FAD
FMN
NAD^+
NADH
$NADP^+$
NADPH
Oxidized glutathione
Quinolinate
Reduced glutathione

Miscellaneous metabolites
2,3-Dihydroxybenzoate
Agmatine
APS
Choline
Geranyl-PP
myo-Inositol
p-Hydroxybenzoate
Putrescine
Spermidine
trans, trans-Farnesyl-PP

Metabolites that are unstable or for other reasons could not be reliably measured using the present method are marked in italics. Those metabolites that could be quantified from *E. coli* extracts are highlighted in bold. *Abbreviations*: P, phosphate; PP, diphosphate. A collective name was assigned to describe isomers that were explicitly studied and could not be differentiated by product ion or retention time (see Table S-1 for details).

raphy columns tested are listed in Table 2 along with the names of their suppliers. All the columns are stable in 100% aqueous mobile phase.

2.2. Compounds and nomenclature

Table 1 lists the 164 known components of cellular metabolism targeted in this study. The compounds are referred to

Table 2
Chromatography columns and conditions tested

Column name (supplier[a])	Column type (abbreviation)	Dimensions, particle size	Chromatography mode tested[b]	pH stability of column	pH tested
Synergi Fusion – RP (Phenomenex)	C18 with embedded polar group (EPG)	250 mm × 2 mm, 4 μm	RP	1–10	2.8, 5.8, 9.0
Synergi Polar – RP (Phenomenex)	Ether linked phenyl (PH)	250 mm × 2 mm, 4 μm	RP	1.5–7	2.8, 5.8
Hypercarb (Thermo)	Porous graphitized carbon (PGC)	100 mm × 2 mm, 5 μm	RP	1–14	2.8, 9.0
Atlantis – HILIC (Waters)	Silica (SiO_2)	150 mm × 2 mm, 5 μm	HILIC	1–6	2.8, 5.8
Luna NH2 (Phenomenex)	Aminopropyl (NH_2)	250 mm × 2 mm, 5 μm	RP, HILIC	1.5–11	2.8, 9.0
Luna CN (Phenomenex)	Cyanopropyl (CN)	250 mm × 2 mm, 5 μm	RP, HILIC	1.5–7	2.8, 5.8
TSK Gel Amide 80 (Tosoh Biosciences)	Carbamoyl (Amide)	250 mm × 2 mm, 5 μm	HILIC	2–7.5	2.8, 5.8

[a] Phenomenex is located in Torrance, CA; Thermo in San Jose, CA; Water in Milford, MA; and Tosoh Biosciences in Montgomeryville, PA.
[b] RP, reverse phase; HILIC, hydrophilic interaction chromatography; flow rate was 150 μL/min.

using their primary names as designated in the Ecocyc database, a comprehensive reference for *E. coli* metabolic processes that can be readily searched for synonyms [8]. Isomers of ∼30% of these metabolites are also known components of metabolism as described in Table S-1. For consistency within the text, we refer to a particular molecular formula using only the name of the isomer that constitutes our purified standard, although other isomers may also be detected at the same retention time using the same SRM. In the cases when we have purified standards corresponding to different isomers of a given metabolite molecular formula, we treat these isomers as independent entities if they can be distinguished using our final LC–MS/MS method; otherwise, we refer to them using a name that encompasses the class of indistinguishable compounds; e.g., D-hexose phosphate for all isomers of D-fructose-6-phosphate (see Table S-1).

2.3. Instrumentation and MS/MS parameter optimization

Mass spectrometric analyses were performed on a Finnigan TSQ Quantum Ultra triple quadrupole mass spectrometer (Thermo Electron Corporation, San Jose, CA, USA). Column effluent was introduced into the electrospray chamber with a 0.1 mm internal diameter fused silica capillary. Electrospray ionization spray voltage was 3200 V in positive mode and 3000 V in negative mode. Nitrogen was used as sheath gas at 30 psi and as the auxiliary gas at 10 psi, and argon as the collision gas at 1.5 mTorr, with the capillary temperature 325 °C. Scan time for each SRM transition was 0.1 s with a scan width of 1 *m*/*z*. The mass spectrometer syringe pump was used to infuse purified compounds in 50:50 methanol:water at 20 μL/min for MS/MS parameter determination using the triple quadrupole instrument's automated fragmentation optimization routine [25]. These studies were carried out for each metabolite in both positive and negative ionization mode. For each metabolite, the ionization mode and SRM parameters of collision energy and product ion mass were selected to optimize the signal-to-noise ratio while also attempting to differentiate isomeric or isobaric compounds by product ion mass. After completing MS/MS parameter optimization, LC–MS/MS was performed using a LC-10A HPLC system (Shimadzu, Columbia, MD, USA) coupled to the mass spectrometer. LC conditions included autosampler temperature 4 °C, column temperature 15 °C, injection volume 10 μL, and solvent flow rate 150 μL/min.

2.4. Parallel chromatography optimization

A 1 μg/mL mixture of standard metabolites was analyzed under each of the 18 different chromatography conditions listed in Table 2. At total of 142 compounds were included in this effort, with 22 of the 164 compounds listed in Table S-2 of the Supplementary Materials omitted from LC optimization either due to poor stability or because the compound was acquired after the optimization data had already been collected. A total of three LC–MS/MS runs (two in positive and one in negative mode) were conducted for each chromatography condition of interest, with each run assessing ∼50 different metabolites using the SRM parameters previously optimized for their detection. Because each SRM scan event takes 0.1 s, the measurement of ∼50 metabolites in any given chromatography optimization run resulted in one SRM scan per compound per ∼5 s chromatography interval, which proved to be adequate peak coverage for assessing chromatography quality. Of note, once the chromatography method is fixed and compound retention times are known, a larger number of analytes can be measured in a single LC–MS/MS run, by conducting the SRM scan associated with a given analyte only during the time interval over which that analyte is known to elute from the LC column.

The LC solvents used for this optimization work were Solvent A: aqueous buffer; Solvent B: methanol for reversed-phase liquid chromatography (RPLC), and acetonitrile for hydrophilic interaction chromatography (HILIC). The selection of methanol for RPLC and acetonitrile for HILIC was based on preliminary experiments in which both solvents were tested in both modes for a number of different columns and pH values. The Solvent A aqueous buffer was selected from 20 mM formic acid in water (pH 2.8); 10 mM ammonium acetate in water with acetic acid

added to adjust acidity (pH 5.8); or 50 mM ammonium acetate in water with ammonium hydroxide added to adjust basicity (pH 9.0). Flow rate was 150 μL/min. The gradient for RPLC was: $t = 0$, 0% B; $t = 30$ min, 100% B; $t = 42$ min, 100% B; $t = 44$ min, 0% B; $t = 50$ min, 0% B. For HILIC, the gradient was: $t = 0$, 100% B; $t = 30$ min, 0% B; $t = 42$ min, 0% B; $t = 44$ min, 100% B; $t = 50$ min, 100% B.

To facilitate selection of potential chromatography conditions for separating numerous metabolites, chromatography performance scores for individual metabolites were determined based on the following parameters: sensitivity (as indicated by natural log of the signal-to-noise ratio at 1 μg/mL analyte concentration), peak sharpness (as indicated by natural log of the peak height; peak height provides a convenient measure of peak sharpness as it is linearly proportional to inverse peak width for Gaussian peaks), peak symmetry (as indicated by the tailing factor, with 1 = tailing factor greater than 4 or no defined peak shape, 2 = tailing factor between 2 and 4, and 3 = tailing factor <2), and retention (with 1 = less than 1.5× void volume, 2 = between 1.5× and 2.5× void volume, and 3 = greater than 2.5× void volume). The cumulative score for each compound is defined by the following product.

$$\text{Score}_{\text{cumulative}} = \text{Score}_{\text{sensitivity}} \times \text{Score}_{\text{peak sharpness}} \times \text{Score}_{\text{peak symmetry}} \times \text{Score}_{\text{retention}}$$

To facilitate analysis of the scores, the following heuristic was used: a good score is >500 (corresponding to signal-to-noise of 1000 at 1 μg/mL, a peak height of 3000, tailing factor <2, retention >2.5× void volume), a fair score is between 250 and 500, and a poor score is <250.

2.5. Optimized LC conditions for aminopropyl column

The LC solvents for the optimized amino-column method are Solvent A: 20 mM ammonium acetate + 20 mM ammonium hydroxide in 95:5 water:acetonitrile, pH 9.45; Solvent B: acetonitrile. The gradients are as follows: positive mode—$t = 0$, 85% B; $t = 15$ min, 0% B; $t = 28$ min, 0% B; $t = 30$ min, 85% B; $t = 40$ min, 85% B; and negative mode—$t = 0$, 85% B; $t = 15$ min, 0% B; $t = 38$ min, 0% B; $t = 40$ min, 85% B; $t = 50$ min, 85% B. Once we finalized the chromatography method, the LC runs were divided into time segments, with the SRM scans within each time segment limited to those compounds eluting during that time internal. Time segments are five segments in positive mode: 0–11, 11–13, 13–15, 15–19, and 19–40 min; and four segments in negative mode: 0–19, 19–24, 24–32, and 32–50 min. For compounds eluting at the boundaries between time segments, the SRM scan corresponding to the compound is conducted in both time segments. Column lifetime for the present method is ∼500 h of running time, after which retention times decrease, especially for phosphate-containing compounds.

2.6. Method validation for purified metabolites

Stability studies were conducted as described in Lu et al. [25], with the exception that the compound concentration was 2 μg/mL and that, for compounds not stable at pH 2.8 (the condition tested in Lu et al. [25]), an additional stability study was run at pH 6.8 (in 0.3% ammonium acetate). Limit of detection, linearity, and reproducibility studies were also conducted as described in Lu et al. [25], with the following modifications: (a) the compound concentrations for linearity and limit of detection studies were 1900, 1500, 1000, 500, 250, 100, 50, 25, 10, 5, 2.5, and 1 ng/mL; (b) data obtained at 1900 ng/mL were omitted from linearity analysis as signal saturation was observed at 1900 ng/mL for several compounds; (c) the compound concentration for reproducibility studies was 1 μg/mL; (d) for seven compounds (indicated in Table S-2), area measurements were used instead of height because run-to-run fluctuations in peak shape resulted in poor peak height reproducibility (for the other compounds, height was used because of ease of data analysis); (e) the internal standard was *N*-acetyl-glutamine at 500 ng/mL; and (f) additional internal standards included in the reproducibility studies were isotope-labeled alanine (SRM: 94 → 47 at 11 eV), glutamate (SRM: 154 → 89 at 15 eV), deoxyadenosine (SRM: 267 → 146 at 20 eV), UMP (SRM: 336 → 102 at 12 eV), and AMP (SRM: 363 → 146 at 21 eV) in positive mode and succinate (SRM: 119 → 74 at 10 eV), threonine (SRM: 123 → 77 at 12 eV), thymidine (SRM: 253 → 132 at 15 eV), TTP (SRM: 493 → 159 at 31 eV), and ATP (SRM: 521 → 423 at 21 eV) in negative mode. Normalization to these internal standards gave similar results to *N*-acetyl-glutamine, with no major improvement in reproducibility even for those compounds that were being compared directly to an isotope-labeled form of the identical compound.

2.7. Bacterial strain and culture conditions

E. coli strain NCM3722 was used for all biological experiments. The cells were grown in shaker flasks at 37 °C in a minimal salts media [26,27] with 10 mM ammonium chloride as the nitrogen source and 0.4% glucose as the carbon source unless otherwise indicated. Exponential-phase cultures were quenched and extracted when optical density at 650 nm (A_{650}) reached ∼0.3. To produce carbon-starved, stationary-phase cultures, *E. coli* were grown in 0.05% glucose media for ∼22 h. The A_{650} of carbon-starved cultures produced in this manner was ∼0.3. To produce uniformly ^{13}C-labeled extracts, *E. coli* maintained on a minimal media plate with uniformly ^{13}C-labeled glucose as the sole carbon source were grown in liquid media utilizing uniformly [^{13}C]glucose.

To determine the differences between the metabolomes of exponentially growing versus carbon-starved, stationary-phase cultures, three flasks of cells were grown under each of the following conditions: unlabeled glucose, exponential phase; [^{13}C]glucose, exponential phase; unlabeled glucose, stationary phase; [^{13}C]glucose, stationary phase. Three samples for LC–MS/MS analysis were prepared by mixing 1:1 unlabeled glucose exponential phase extract and [^{13}C]glucose stationary phase extract, and three samples were prepared by mixing 1:1 [^{13}C]glucose exponential phase extract and unlabeled glucose stationary phase extract. Each peak height from the resulting data set was corrected for minor variations in culture density

by dividing the peak height of the individual isotopic (^{12}C- or ^{13}C-) form of metabolite by the A_{650} of the specific [^{12}C]- or [^{13}C]glucose culture used to generate the sample.

2.8. Metabolite extraction

Metabolites were serially extracted essentially as described in Lu et al. [25]. In brief, bacteria were pelleted by centrifugation for 4 min at 5000 × *g*, the supernatant was aspirated, and 300 μL of 80:20 methanol:water at dry ice temperature (−75 °C) was added to the pellet and mixed. After 15 min at −75 °C, the sample was spun in a micro-centrifuge at 13,200 rpm for 5 min at 4 °C and the soluble extract was removed. The pellet was then re-suspended again in 80:20 methanol:water, placed on dry ice for 15 min, and centrifuged to yield a second clear extract, which was combined with the first extract. The pellet was then again re-suspended in 80:20 methanol:water and the resulting suspension was sonicated in an ice bath for 15 min using a FS30H Ultrasonic Cleaner (Fisher Scientific, Pittsburgh, PA, USA) with a power of 100 W at 42 kHz. The sample was then again spun down and the resulting soluble phase combined with the initial two extracts to give a total of 700 μL of extract. In certain cases, before analysis, the extract was mixed with purified standards and/or isotope-labeled extract as indicated.

3. Results

3.1. Optimization of MS/MS parameters

A required initial step in developing an LC–MS/MS assay employing SRM detection is determination of the best daughter ion to monitor for each analyte of interest. In addition, it is desirable to optimize the collision energy for producing that daughter ion. The major daughter ions for each of the 164 purified metabolites studied here was determined by using the automated fragmentation optimization routine of our triple quadrupole instrument while infusing a solution containing the metabolite directly into its electrospray ionization source. The optimized SRM parameters for each metabolite are provided in Table S-2 of the Supplementary Materials. Probable product ion molecular formulas, which define the product mass for isotope-labeled metabolites, were determined as described earlier [25] and are provided also in Table S-2.

3.2. Chromatography optimization

A primary goal of the present work was to identify a single LC condition that enables efficient analysis of as many known, water soluble intracellular metabolites as possible. To the end, mass spectrometry detection was used to determine typical chromatography parameters, such as peak shape, retention time, and signal-to-noise, for numerous different analytes in a single LC run. Overall, chromatography quality was assessed for the 18 different conditions listed Table 2 for 142 different metabolites.

The selection of chromatography conditions was based primarily on the hydrophilic nature of most of the analytes of interest. Methods involving the use of non-volatile salts were avoided to reduce risk of ion suppression. The methods investigated can be divided into RPLC versus HILIC. The RPLC methods included both a minor variant of a standard C18-column that employs an embedded polar group to attempt to improve separation of hydrophilic compounds [28] and columns that have recently been reported in the literature to have value for analysis of polar compounds, such as porous graphitized carbon [29]. The HILIC columns ranged from a negatively charged stationary phase (silica) to a positively charged one (amino) [30]. Uncharged columns tested in HILIC mode included cyano (hydrogen bond acceptor but not donor) and amide (hydrogen bond acceptor and donor). A spectrum of pH values was tested for each column and chromatography mode. Of note, to avoid complicating this already intensive chromatography optimization effort, ion-pairing was not explored despite its known utility in enhancing the reversed-phase retention of hydrophilic analytes.

Some of the major trends observed in the chromatography optimization data are highlighted by the behavior of three example compounds shown in Fig. 1. Many compounds were only minimally retained with the RPLC methods. In addition, the RPLC methods, likely due to the lack of phosphate in the running buffer and our decision not to explore ion pairing reagents, generally yielded poor peak shape or no detectable peak for highly phosphorylated compounds such as triphosphates. Better retention was generally obtained in HILIC mode. Among HILIC approaches, the cyano column at acidic pH yielded outstanding chromatography for many amines, but minimal retention of many others compounds. In addition, both the silica and cyano columns yielded very poor peak shape or no detectable peak for multiply phosphorylated compounds. In contrast, the amide and amino columns retained and gave detectable peaks for most compounds including triphosphates, with peak shape generally better for the amino column at pH 9 than the amide column at pH 6. Of note, the amide column could not be tested at pH 9 due to its lack of stability in base.

Fig. 1 presents data on a total of three compounds under six chromatography conditions (i.e., it summarizes 18 compound-specific SRM chromatograms). In total, the present chromatography optimization effort generated more than 100-times this amount of data, a total of 2556 compound-specific SRM chromatograms (142 analytes × 18 conditions). It was thus difficult to get a handle on the overall content of the data by standard visual examination of chromatograms. Hence, a scoring system was devised to provide a shorthand notation for the performance of each compound under each set of chromatography conditions (see Section 2). This scoring system was designed based on empirical heuristics, with clear recognition that certain arbitrary cut-offs are involved. Nevertheless, the system desirably takes into account sensitivity, peak sharpness, peak symmetry, and retention for each analyte, combining them to yield a cumulative integer score. The scores for all tested compounds in all tested conditions are provided in Table S-3 of the Supplementary Materials.

To further simplify the chromatography optimization data, the score for each compound in each condition was categorized

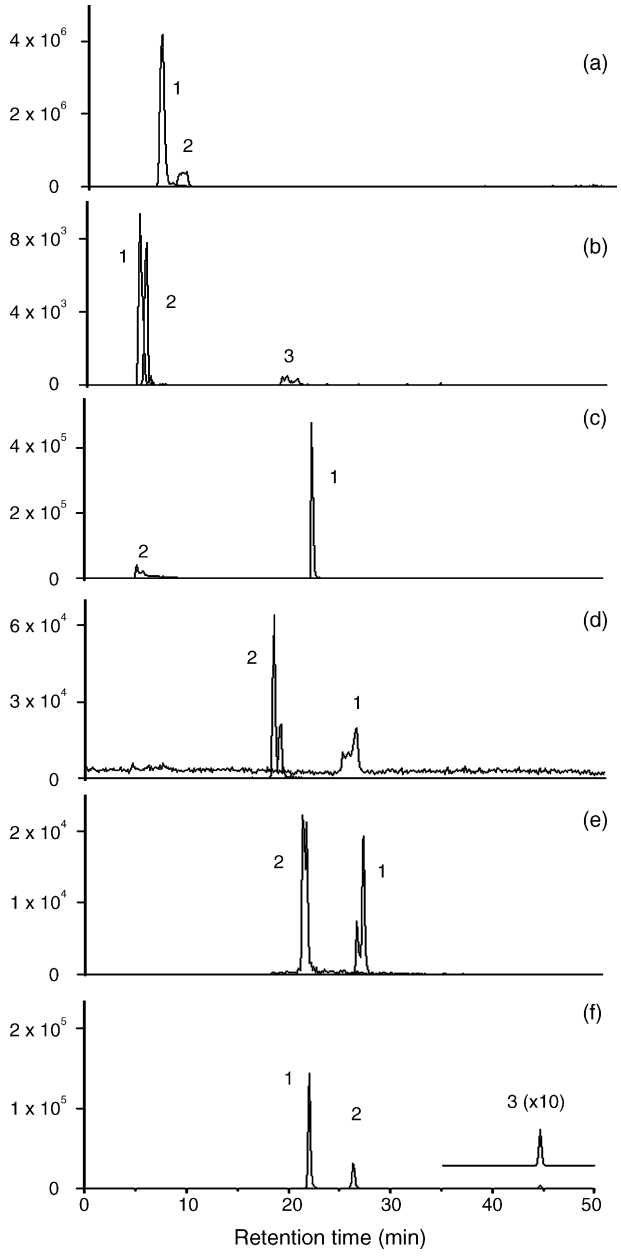

Fig. 1. Typical results obtained during chromatography optimization. Chromatograms are provided for three metabolites as examples: 1 = glucosamine; 2 = allantoic acid; 3 = CTP. *Y*-Axis units are ion counts. Note that CTP was not detectable in many conditions. (a) C18 column with embedded polar group in reversed-phase mode at pH 2.8. (b) Aminopropyl column in reversed-phase mode at pH 9. (c) Cyanopropyl column in HILIC mode at pH 2.8. (d) Silica column in HILIC mode at pH 5.8. (e) Amide column in HILIC mode at pH 5.8 (CTP was detectable, but is hidden between glucosamine and allantoic acid). (f) Aminopropyl column in HILIC mode at pH 9.

as poor, fair, or good. The cut-offs defining these groups were set by comparing chromatographic performance of a few metabolites to their scores. Examples in Fig. 1 of "good" performance are peak 1 in chromatograms (c) and (f). "Fair" performers include peak 1 in chromatogram (a) (good signal and shape but poor retention); peaks 1 and 2 in chromatogram (e) (good signal and retention but splitting); and peaks 2 and 3 in chromatogram (f) (good retention and shape but suboptimal signal). "Poor" performers include peak 3 in chromatogram (b) and those cases in which CTP was not detected at all.

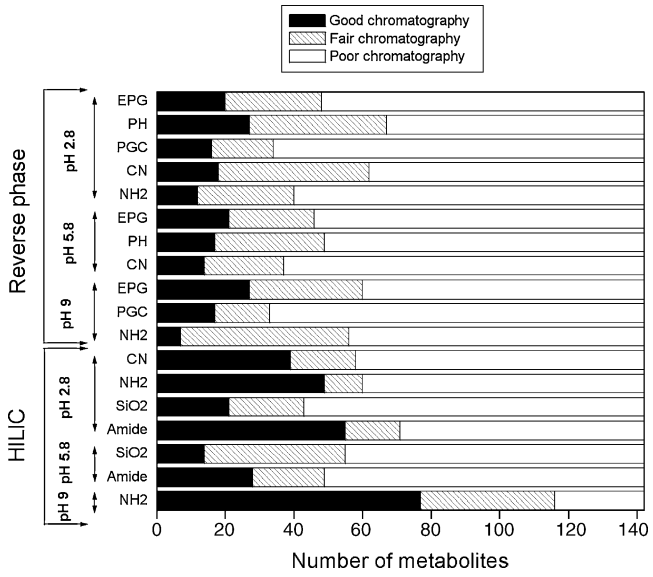

Fig. 2. Summary of chromatography optimization results. The performance of each chromatography condition was classified as good, fair, or poor for each of 142 different metabolite standards as described in Section 2. Chromatography columns are described in Table 2. In brief, EPG is C18 with an embedded polar group; PH, phenyl; PGC, porous graphitized carbon; CN, cyanopropyl; NH_2, aminopropyl; SiO_2, silica.

The overall performance of the different sets of chromatography conditions tested, as evaluated by individual metabolite's chromatography performance score, is shown in Fig. 2. Among all the conditions, amino column at pH 9 in HILIC mode produced favorable results for the largest number of metabolite, yielding a good chromatography score for 77 metabolites and fair chromatography score for 39 metabolites (total 116 out of 142 studied metabolites). Thus, we elected to develop the preliminary amino column method further.

3.3. Finalization of LC–MS/MS method

Having identified HILIC with an amino column at pH 9 as a promising general chromatography approach, the effect of subtle changes in pH and solvent gradient were assessed. Slightly more basic conditions resulted in more rapid and reliable elution of strongly retained species (e.g., triphosphates) without compromising overall performance. A 15 min gradient from acetonitrile into water adequately balanced separation speed versus efficiency. Final LC parameters are provided in Section 2.

With the LC parameters finalized, the retention time for each compound was determined. We then used knowledge of these retention times to divide the chromatography run into different time segments, with SRM scans within any particular segment limited to those compounds eluting during that time interval. By dividing a single LC run in this manner, all of the compounds of interest can be measured in only two LC runs, one in positive and one in negative mode, while retaining adequate peak coverage. Thus, the final method for the 164 compounds of interest involves two LC runs that together take 90 min.

3.4. Method performance for purified compounds

The method effectively separates metabolites, as highlighted by the example chromatograms shown in Fig. 3 and distribution of retention times shown in Fig. 4a. It also detects most metabolites with good sensitivity, as shown in Fig. 4b, with a median limit of detection (LOD; defined as the lowest concentration at which the signal-to-noise ratio is larger than 5) of 25 ng/mL, and >90% of the metabolites having an LOD < 1 μg/mL (Table S-2).

Before assessing the quantitative reliability (linearity and reproducibility) of the method, the stability of each of the 164 metabolites was determined (Table S-2). It was found that 143 of the compounds are stable at pH 2.8, as defined by less than 20% decay over one week of storage at 4 °C. Among the 21 compounds that are unstable at pH 2.8, 11 are stable at pH 6.8. Those compounds that were unstable at both pHs 2.8 and 6.8 were omitted from further analyses.

The quantitative capabilities of the amino column method were determined for the stable metabolites that could be detected with a LOD ≤1 μg/mL (total 144 compounds). Linearity was determined in the range from each metabolite's LOD up to 1.5 μg/mL. Linearity data for every compound is provided in Table S-2. For all but one compound, R^2 was >0.9, with the median $R^2 > 0.99$. Intra- and inter-day assay reproducibility was also determined for a mixture containing the 144 compounds of interest. The relative standard deviation (RSD) for repetitive sample analysis, both intra- and inter-day, was <35% for all but two compounds, with the median intra-day RSD 10%, and the median inter-day RSD also 10% (see Table S-2 for individual compound values). Excluding the compounds with unacceptable linearity or reproducibility, a total of 141 compounds gave quantitative data.

The effect of the solvent used to dissolve the standards on LC–MS/MS performance was also briefly assessed. Indistinguishable results were obtained for standard mixtures dissolved in acetonitrile:water and methanol:water, for aqueous fractions from 0 to 50%. Higher aqueous fractions were not tested.

To assess the effect of salts on chromatography and/or ionization, standards dissolved in 50:50 methanol:water were

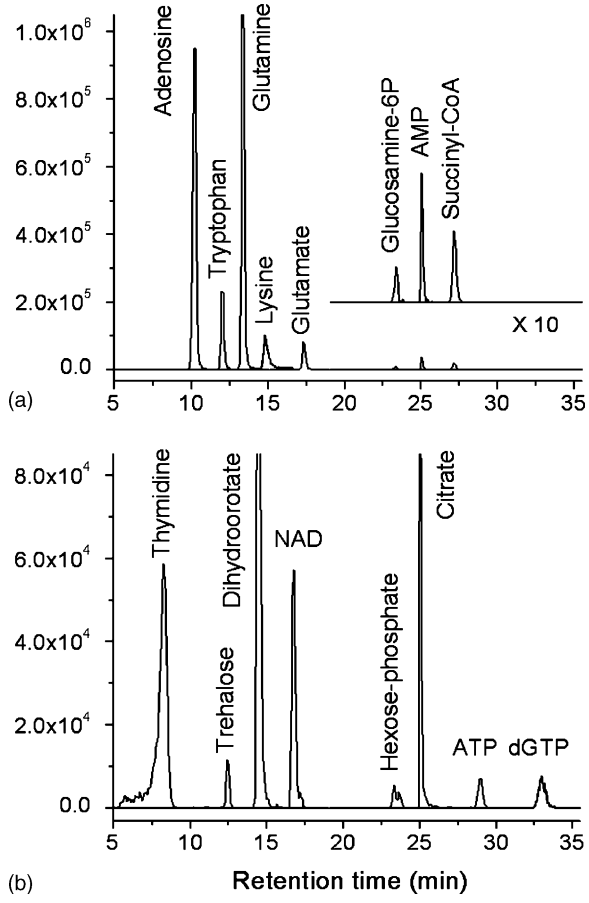

Fig. 3. Example chromatograms of purified metabolite standards. (a) Overlay of the chromatograms produced by SRM-based measurement of the indicated eight compounds (each at 1 μg/mL) detected in positive ion mode. *Y*-Axis units are ion counts. (b) Analogous data from negative mode. Note that the individual chromatograms corresponding to a single SRM generally contain only a single peak. An exception is that SRM *m/z* 147 → 84 detects both glutamine and lysine, which are well-resolved chromatographically.

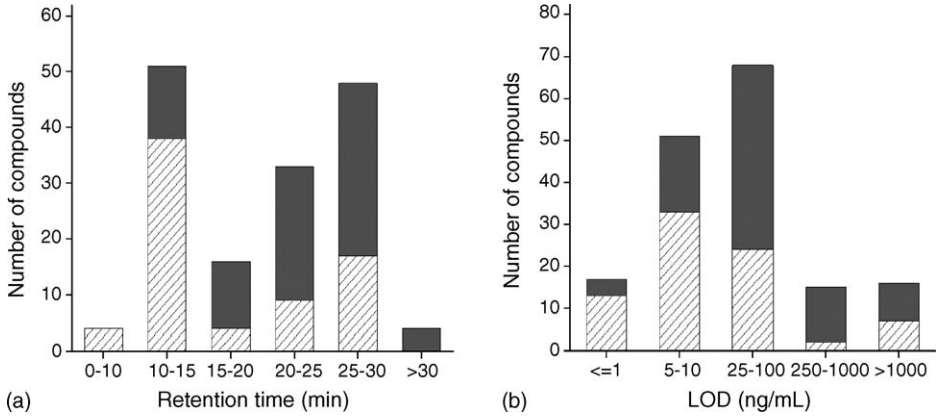

Fig. 4. Separation power and sensitivity of the LC–MS/MS method. (a) Histogram of the distribution of retention times of the 156 metabolites detectable using final LC–MS/MS method. (b) Histogram of the distribution of the limit of detection (LOD) for all 164 compounds investigated here. Slashes indicate compounds detected in positive mode and solid gray indicates compounds detected in negative mode.

spiked with sodium chloride and analyzed. Sodium chloride concentrations up to ∼20 mM also did not affect method performance. Salt concentrations in the range of ∼100 mM resulted in discernable (typically ∼two-fold) ion suppression for chromatography peaks with retention times of ∼13–16 min. These peaks apparently co-elute with salt. Substantially higher salt concentrations (e.g., >500 mM) resulted in more severe ion suppression, again especially around 13–16 min retention time, as well as peak shape changes for certain compounds.

3.5. Validation of measurements from E. coli extracts

To determine the performance of our method for biological samples, extracts of *E. coli* grown exponentially in minimal media containing either unlabeled (^{12}C) or isotope-labeled [^{13}C]glucose were analyzed. Batch cultures (50 mL) were harvested by centrifugation and metabolites extracted using three serial rounds of 80% methanol:20% water [25]. To search for uniformly ^{12}C- or ^{13}C-forms of the metabolites, SRMs corresponding to both their ^{12}C- and ^{13}C-forms were included. For 79 compounds, peaks eluting at the identical chromatography retention time as the corresponding metabolite standard met the following criteria: the peak corresponding to the ^{12}C-form of the compound was found specifically in the extract of cells grown in ^{12}C- but not [^{13}C]glucose, and likewise for the ^{13}C-peak; and the ^{12}C-peak from the cells grown in [^{12}C]glucose was roughly comparable in size to the ^{13}C-peak from the cells grown in [^{13}C]glucose (Fig. 5). This confirmed that each of these 79 metabolites were indeed synthesized by *E. coli* from glucose introduced into the medium, and that each metabolite contained the anticipated number of carbon atoms. Confirmation of the carbon count of each *E. coli* derived peak was valuable because cells may contain a large diversity of known and unknown metabolites and triple quadrupole mass spectrometry does not provide sufficient mass accuracy for direct determination of their molecular formulas.

To explore the quantitative reproducibility of analysis of cellular extracts with the present LC–MS/MS method, a particular ^{12}C-extract was analyzed multiple times over a 24 h period, with the extract stored at 4 °C between injections. One compound, CoA, was clearly unstable in the cell extract despite being stable on its own in solution, and nine compounds, generally having undesirably small signals, yielded erratic data; these compounds were omitted from further analyses. Data for the remaining 69 compounds are provided in Table 3, with the median RSD for repeated analysis of the same extract 13%.

To determine the overall reproducibility of measurement of the *E. coli* metabolome using the present approach, independent cell extracts obtained from independent cultures grown under identical conditions were analyzed. The median inter-extract RSD was found to be 31%. Thus, sample-to-sample variability is a somewhat more important contributor to overall variability than imprecise LC–MS/MS measurement.

3.6. Effect of carbon-starvation on the E. coli metabolome

The ability to effectively label *E. coli*'s metabolome with [^{13}C]glucose enabled exploration of the metabolome of exponentially growing *E. coli* versus *E. coli* driven into stationary phase by carbon starvation for ∼20 h. Extracts of exponential phase *E. coli* fed [^{12}C]glucose were mixed with extracts of stationary phase *E. coli* fed [^{13}C]glucose, and vice versa. The resulting measurements of metabolites from exponential growing cells (a total of three ^{12}C- and three ^{13}C-measurements)

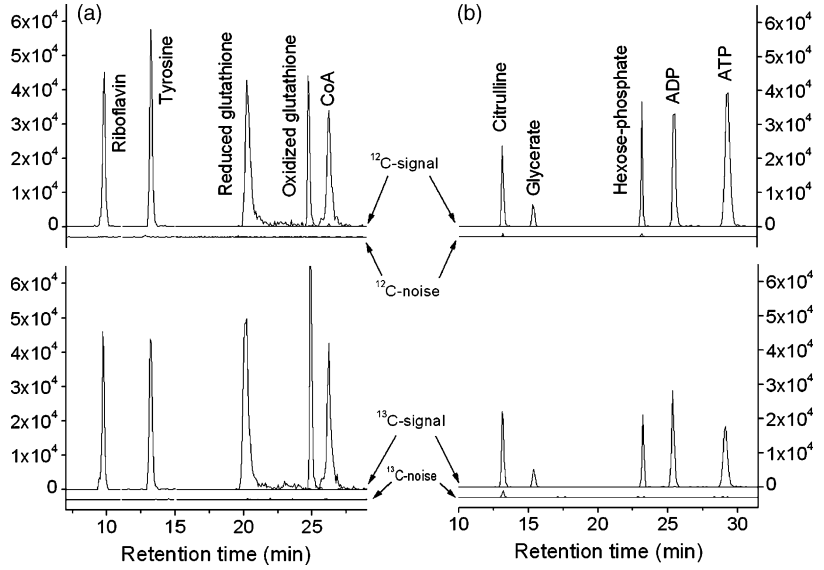

Fig. 5. Confirmation of measurement specificity in *E. coli* extract using isotope-labeling. The upper plots show the results of SRM scans corresponding to the uniformly ^{12}C-forms of the indicated metabolites. The lower plots show the results for scans corresponding to the uniformly ^{13}C-forms of those same metabolites. Within each plot, the upper trace shows data from cells grown in the carbon source matched to the SRM scans (i.e., [^{12}C]glucose for the upper plots and [^{13}C]glucose for the lower plots), whereas the lower trace, marked "noise", refers to data from cells grown in the mismatched carbon source. Units of the *Y*-axis are ion counts; for ease of viewing, the noise traces have been shifted down by ∼3000 ion counts. (a) Representative data for metabolites analyzed in positive ionization mode. (b) Analogous data for metabolites analyzed in negative ionization mode.

Table 3
Intra- and inter-sample variation in metabolite signal intensities in *E. coli* extracts

Metabolite	Parent ion formula[a]	^{12}C parent mass	^{12}C signal intensity[b]	^{12}C noise (%)[c]	^{13}C signal intensity[b]	^{13}C noise (%)[c]	% RSD Intra-sample	% RSD Inter-sample
Glycine	$C_2H_6NO_2^+$	76	4.3E+03	9.3	5.6E+03	0.4	16	54
Alanine	$C_3H_8NO_2^+$	90	4.9E+05	0.5	8.0E+05	0.0	7	27
Glycerate	$C_3H_5O_4^-$	105	6.0E+03	0.1	4.8E+03	0.1	16	63
Fumarate	$C_4H_3O_4^-$	115	5.4E+03	3.6	3.6E+03	2.8	25	59
Proline	$C_5H_{10}NO_2^+$	116	6.5E+05	0.7	1.0E+06	0.0	5	35
Succinate	$C_4H_5O_4^-$	117	1.5E+05	1.8	1.2E+05	0.1	11	14
Threonine	$C_4H_8NO_3^-$	118	1.9E+04	1.3	2.6E+04	0.0	20	33
Valine	$C_5H_{12}NO_2^+$	118	1.7E+05	0.4	4.0E+05	0.0	5	21
(Iso)leucine	$C_6H_{14}NO_2^+$	132	2.7E+05	2.0	2.5E+05	0.0	5	16
Aspartate	$C_4H_6NO_4^-$	132	1.9E+03	1.6	1.9E+03	3.1	13	25
Asparagine	$C_4H_9N_2O_3^+$	133	1.0E+04	6.7	2.4E+04	1.9	9	20
Malate	$C_4H_5O_5^-$	133	1.3E+05	1.2	1.5E+05	0.4	14	41
Ornithine	$C_5H_{13}N_2O_2^+$	133	4.9E+04	6.1	3.8E+04	0.0	11	31
Adenine	$C_5H_6N_5^+$	136	1.2E+04	2.7	2.4E+04	1.0	9	30
Hypoxanthine	$C_5H_5N_4O^+$	137	3.0E+04	0.1	4.3E+04	0.2	18	27
α-Ketoglutarate	$C_5H_5O_5^-$	145	1.7E+03	10.0	1.5E+03	2.0	22	4
Glutamine	$C_5H_{11}N_2O_3^+$	147	1.8E+05	0.6	2.2E+05	0.0	11	33
Lysine	$C_6H_{15}N_2O_2^+$	147	1.1E+05	1.2	9.7E+04	0.1	9	33
Glutamate	$C_5H_{10}NO_4^+$	148	1.8E+06	0.1	2.5E+06	0.0	8	23
Methionine	$C_5H_{12}NO_2S^+$	150	2.4E+04	1.8	5.5E+04	0.4	11	32
Guanine	$C_5H_6N_5O^+$	152	3.1E+04	0.1	3.4E+04	1.8	26	36
2,3-Dihydroxybenzoate	$C_7H_5O_4^-$	153	6.1E+04	0.0	1.9E+04	0.1	23	40
Histidine	$C_6H_{10}N_3O_2^+$	156	1.6E+04	6.9	9.4E+03	0.3	16	32
Phenylalanine	$C_9H_{12}NO_2^+$	166	1.1E+05	1.7	8.7E+04	0.0	8	19
Phosphoenolpyruvate	$C_3H_4O_6P^-$	167	1.7E+04	0.4	1.0E+04	0.0	6	32
Arginine	$C_6H_{13}N_4O_2^-$	173	1.3E+04	0.3	1.1E+04	0.2	23	15
Aconitate	$C_6H_5O_6^-$	173	9.4E+03	1.3	3.3E+03	0.5	15	32
Citrulline	$C_6H_{12}N_3O_3^-$	174	1.7E+04	2.7	1.7E+04	9.3	21	31
Tyrosine	$C_9H_{12}NO_3^+$	182	4.4E+04	0.5	3.4E+04	1.7	10	25
3-Phosphoglycerate	$C_3H_6O_7P^-$	185	7.7E+04	0.2	3.5E+04	0.6	11	28
Citrate	$C_6H_7O_7^-$	191	1.2E+05	2.1	5.0E+04	5.8	11	26
Tryptophan	$C_{11}H_{13}N_2O_2^+$	205	2.8E+04	1.0	2.2E+04	0.1	12	36
D-Rib(ul)ose-5-phosphate	$C_5H_{10}O_8P^-$	229	4.6E+03	1.6	2.3E+03	3.6	22	22
Thymidine	$C_{10}H_{13}N_2O_5^-$	241	3.3E+02	6.0	8.2E+02	0.3	27	47
Uridine	$C_9H_{11}N_2O_6^-$	243	7.5E+02	1.7	1.2E+03	1.0	31	72
Cytidine	$C_9H_{14}N_3O_5^+$	244	3.1E+03	0.5	5.4E+03	1.1	5	50
Deoxyadenosine	$C_{10}H_{14}N_5O_3^+$	252	2.7E+03	1.7	3.2E+03	1.4	25	16
D-Hexose-phosphate	$C_6H_{12}O_9P^-$	259	3.4E+04	1.2	1.5E+04	0.1	11	26
Glucosamine-6-P	$C_6H_{15}NO_8P^+$	260	5.8E+03	2.7	1.1E+04	0.3	26	23
Adenosine	$C_{10}H_{14}N_5O_4^+$	268	3.6E+04	0.1	1.4E+05	0.0	7	58
Inosine	$C_{10}H_{13}N_4O_5^+$	269	8.4E+03	0.1	1.4E+04	0.0	10	41
Guanosine	$C_{10}H_{14}N_5O_5^+$	284	1.9E+04	0.2	1.8E+04	0.5	17	33
dCMP	$C_9H_{15}N_3O_7P^+$	308	4.3E+03	1.8	5.1E+03	0.6	18	27
dTMP	$C_{10}H_{16}N_2O_8P^+$	323	5.1E+03	1.3	4.3E+03	2.1	21	18
CMP	$C_9H_{15}N_3O_8P^+$	324	2.6E+04	2.4	2.2E+04	0.1	17	19
UMP	$C_9H_{14}N_2O_9P^+$	325	1.4E+04	0.2	1.4E+04	0.0	9	9
Cyclic-AMP	$C_{10}H_{11}N_5O_6P^-$	328	1.5E+03	1.7	1.3E+03	0.2	24	65
dAMP	$C_{10}H_{15}N_5O_6P^+$	332	1.2E+04	0.6	1.2E+04	2.2	19	16
Fructose-1,6-bisphosphate	$C_6H_{13}O_{12}P_2^-$	339	1.4E+05	0.7	4.4E+04	3.6	14	32
AMP	$C_{10}H_{15}N_5O_7P^+$	348	2.4E+05	0.0	2.4E+05	0.4	11	23
IMP	$C_{10}H_{14}N_4O_8P^+$	349	5.5E+04	0.1	5.5E+04	0.1	9	26
GMP	$C_{10}H_{15}N_5O_8P^+$	364	3.5E+04	0.2	2.2E+04	0.2	18	10
Riboflavin	$C_{17}H_{21}N_4O_6^+$	377	3.2E+04	0.2	3.9E+04	0.1	11	24
S-Adenosyl-L-methionine	$C_{15}H_{23}N_6O_5S^+$	399	6.3E+04	0.0	7.8E+04	0.0	10	30
dTDP	$C_{10}H_{15}N_2O_{11}P_2^-$	401	2.9E+03	0.7	6.7E+03	0.3	15	49
CDP	$C_9H_{14}N_3O_{11}P_2^-$	402	4.9E+03	0.2	9.6E+03	1.9	11	32
UDP	$C_9H_{13}N_2O_{12}P_2^-$	403	1.3E+04	0.3	8.3E+03	1.6	12	33

Table 3 (*Continued*)

Metabolite	Parent ion formula[a]	^{12}C parent mass	^{12}C signal intensity[b]	^{12}C noise (%)[c]	^{13}C signal intensity[b]	^{13}C noise (%)[c]	% RSD Intra-sample	% RSD Inter-sample
ADP	$C_{10}H_{14}N_5O_{10}P_2^-$	426	3.4E+04	0.0	2.1E+04	0.1	12	18
TTP	$C_{10}H_{16}N_2O_{14}P_3^-$	481	1.7E+03	0.8	2.6E+03	0.8	18	36
CTP	$C_9H_{15}N_3O_{14}P_3^-$	482	4.8E+03	0.2	2.6E+03	0.8	18	41
UTP	$C_9H_{14}N_2O_{15}P_3^-$	483	9.1E+03	0.1	6.4E+03	0.2	14	36
ATP	$C_{10}H_{15}N_5O_{13}P_3^-$	506	3.4E+04	0.1	1.2E+04	1.4	10	31
UDP-D-glucose	$C_{15}H_{23}N_2O_{17}P_2^-$	565	1.0E+05	0.0	6.4E+04	0.0	15	36
UDP-*N*-acetyl-D-glucosamine	$C_{17}H_{26}N_3O_{17}P_2^-$	606	2.8E+04	0.0	3.3E+04	0.0	7	22
Oxidized glutathione	$C_{20}H_{33}N_6O_{12}S_2^+$	613	5.5E+04	0.0	1.7E+05	0.0	31	41
NAD^+	$C_{21}H_{26}N_7O_{14}P_2^-$	662	2.0E+05	0.0	1.6E+05	0.0	11	31
$NADP^+$	$C_{21}H_{27}N_7O_{17}P_3^-$	742	1.1E+05	0.0	5.7E+04	0.0	18	19
FAD	$C_{27}H_{34}N_9O_{15}P_2^+$	786	7.9E+03	0.2	9.5E+03	0.3	18	25
Acetyl-CoA	$C_{23}H_{39}N_7O_{17}P_3S^+$	810	1.9E+05	0.1	2.2E+05	0.0	8	15

[a] +, Indicates protonated ion detected in positive mode; − indicates deprotonated ion detected in negative mode; parent mass refers to the ionized form.
[b] Mean signal intensity ($N = 3$).
[c] The term ^{12}C-noise refers to the ^{12}C-signal for cells grown in ^{13}C-glucose; the term ^{13}C-noise is analogously the ^{13}C-signal for cells grown in unlabeled glucose.

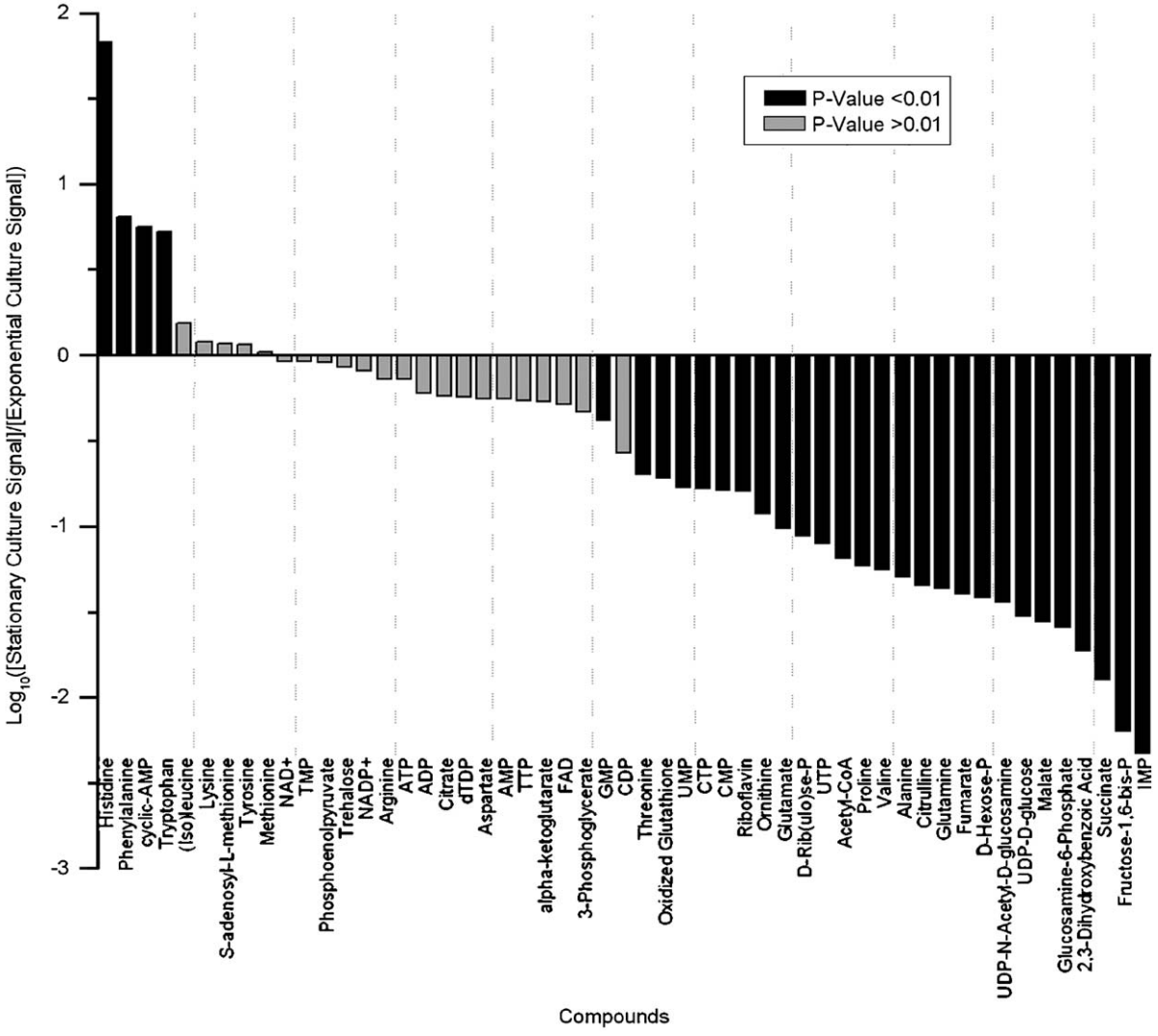

Fig. 6. Effect of carbon-starvation on the *E. coli* metabolome. Plotted are selected metabolome differences between exponentially growing, glucose-fed *E. coli* (exponential culture) versus *E. coli* starved for carbon for ∼20 h (stationary culture). Data represent the average of six independent stationary-phase and exponential-phase cultures.

were compared to the analogous measurements from stationary phase cells obtained during the same LC–MS/MS runs, using two-tailed Student's *T* test. The selected metabolome differences are summarized in Fig. 6. Of note, metabolite levels are very sensitive to changes in cell environment [31]. Hence, the results obtained in this study could be specific to the quenching technique used (centrifugation followed by addition of 80:20 methanol:water at dry ice temperature). With these specific quenching conditions, a majority of the studied metabolites show significant changes upon carbon starvation at the $p < 0.01$ level (with the expected number of false discoveries at this *p*-value less than one), with 35 metabolites significantly decreased and four significantly increased. Many of the observed changes were dramatic in magnitude, with histidine increasing and 19 compounds decreasing by more than an order of magnitude. Most profoundly decreased were the key glycolytic intermediate fructose-1,6-bisphosphate and the *de novo* purine biosynthesis intermediate IMP.

4. Discussion

Mass spectrometry is a powerful tool for metabolomic analysis [32,33]. Though direct infusion has been tried for comparative metabolomics and screening studies [34], chromatographic separation of metabolites [22,35–39] prior to their ionization is desirable for increased measurement specificity and quantitative reliability. Here we use SRM-scanning to optimize chromatography conditions for many compounds in parallel. The data resulting from this chromatography optimization effort, which are presented in Table S-3, provide a useful reference regarding the chromatographic behavior of cellular metabolites on different column chemistries and in different separation modes. We find that amino-column-based separation in HILIC mode is an effective chromatography approach for a diverse set of cellular metabolites that includes many compounds too hydrophilic to separate reliably using typical RPLC methods. A likely reason for the good performance of the amino column in HILIC mode is its ability to retain metabolites through hydrogen bond donor, hydrogen bond acceptor, and ionic interactions [38], with all of these interactions weaker in water than organic solvent, thereby enabling effective elution of the column with water.

Using this LC–ESI-MS/MS method, we are able to quantify reliably 141 of the 164 metabolites under investigation from standard mixtures, and to detect and quantify 69 of these compounds in *E. coli* extracts. The set of compounds detected from *E. coli* of course depends not only on the LC–MS/MS method, but also the cell growth, collection, and extraction conditions. Thus, the present set of 69 compounds quantified should be viewed as a starting point for determining whether the 72 compounds that could not be quantified can be obtained with faster cell harvesting [40–42] or alternative extraction conditions [12,42], appear only in response to specific cell growth conditions [43,44], or perhaps are subject to metabolic channeling [45,46].

With respect to performance of the present method, overall quantitative reliability is comparable to most LC–MS/MS methods, with between sample reproducibility similar to most previous metabolomic approaches [15,18,22,37]. Disadvantages of the present method include its inability to detect compounds not specifically targeted by SRM scan events; failure to separate sugar isomers [22,23,47,48]; poor performance for reduced thiols [19], NADH, and NADPH; worse performance than GC/MS for small, volatile metabolites [22]; and worse sensitivity than reversed-phase LC–MS/MS at acidic pH for many positive-mode compounds [25]. Nevertheless, we believe that for global evaluation of cellular metabolism, these disadvantages are outweighed by advantages of the present method including good separation of most metabolites; measurement of di- and triphosphate compounds which cannot be detected using GC/MS methods [22,49]; and most importantly, quantification of a large number and broad spectrum of unambiguously defined compounds of high biological importance.

The applicability of the present LC–ESI-MS/MS method is highlighted by our results regarding the metabolome of exponentially growing versus carbon-starved *E. coli*, between which we find 39 compounds that differ significantly in amount. Reassuringly, while most compounds decrease during carbon starvation, we find that cyclic-AMP, a known signal for carbon-starvation [50], is increased. Thus, while inter-sample variability is substantial, the present approach is nevertheless effective at recapitulating known effects of carbon starvation, while also identifying many new ones with high statistical certainty.

Many of the observed effects of carbon starvation in *E. coli* parallel those that we previously observed in *S. enterica* using a reversed-phase LC–MS/MS method that quantified a smaller number of compounds [25]. In particular, focusing on amino acids, both studies found significant increases in phenylalanine and decreases in valine, alanine, and glutamine during carbon starvation. Moreover, both studies found significant starvation-induced decreases in riboflavin, glucosamine-6-phosphate, and IMP. These observations suggest the potential existence of a conserved pattern of metabolome remodeling during carbon-starvation.

The present study also investigated a number of compounds that were not analyzed in the previous study of *S. enterica.* These include the central carbon intermediates of D-hexose-phosphate (likely predominantly glucose-6-phosphate), fructose-1,6-bisphosphate, and acetyl-CoA, all of which were not surprisingly found to decrease profoundly in carbon-starvation. Notably, however, comparably impressive decreases in certain other key central carbon compounds, including phosphoenolpyruvate, citrate, and alpha-ketoglutarate were not observed, suggesting the possibility of complex regulation of central carbon metabolism during carbon-starvation.

While the starvation-induced metabolome changes observed here are impressive in their magnitudes and statistical significance, they are only a small first step towards improved understanding of the overall metabolic activity of nutrient-limited microorganisms. One key objective of future research should be to determine whether the present results reliably represent physiology or instead are specific to the present quenching scheme. Other objectives should include understanding the dynamics of the observed metabolome changes, as a next step towards eventually identifying the regulatory events that produce these patterns of intracellular metabolite concentrations.

5. Conclusion

A systematic chromatography optimization approach identified HILIC using an aminopropyl column at pH 9.45 as one effective means of separating polar cellular metabolites prior to their SRM detection on a triple quadrupole mass spectrometer. The resulting LC–MS/MS approach advantageously ensures the identity of each compound being quantified based not just on the compound's molecular weight, but also its retention and fragmentation properties. The quantitative reproducibility of the analytical method itself is respectable (RSDs generally between 10 and 15%), especially given the substantial number of low concentration analytes being measured. Although challenges in minimizing sample-to-sample variability remain, differences between exponentially growing and carbon-starved *E. coli* can be readily determined. Thus, the present LC–MS/MS approach provides a promising new tool for quantitative studies of cellular metabolism.

Acknowledgments

We thank David Botstein, Ned Wingreen, Leonid Kruglyak, Thomas Silhavy, John T. Groves, Sanford Silverman, Matthew Brauer, Melisa Gao, and Haoqian Chen for their support and technical and intellectual contributions to this research. Thanks also to the Lewis-Sigler Institute, Princeton University Department of Chemistry, and the National Institutes of Health, and the Beckman Foundation for funding these efforts.

Appendix A. Supplementary data

Supplementary data associated with this article can be found, in the online version, at doi:10.1016/j.chroma.2006.05.019.

References

[1] R.B. Stoughton, Annu. Rev. Biochem. 74 (2005) 53.
[2] S.G. Oliver, M.K. Winson, D.B. Kell, F. Baganz, Trends Biotechnol. 16 (1998) 373.
[3] J.C. Lindon, et al., Nat. Biotechnol. 23 (2005) 833.
[4] S.J. Wiback, R. Mahadevan, B.Ø. Palsson, Biotechnol. Bioeng. 86 (2004) 317.
[5] C.A. Ouzounis, P.D. Karp, Genome Res. 10 (2000) 568.
[6] R.U. Ibarra, J.S. Edwards, B.Ø. Palsson, Nature 420 (2002) 186.
[7] S.S. Fong, B.Ø. Palsson, Nat. Genet. 36 (2004) 1056.
[8] I.M. Keseler, J. Collado-Vides, S. Gama-Castro, J. Ingraham, S. Paley, I.T. Paulsen, M. Peralta-Gil, P.D. Karp, Nucleic Acids Res. 33 (2005) D334.
[9] J. Nielsen, S. Oliver, Trends Biotechnol. 23 (2005) 544.
[10] F.C. Neidhardt, J.L. Ingraham, M. Schaechter, Physiology of the Bacterial Cell: A Molecular Approach, Sinauer Associates, Sunderland, MA, 1990.
[11] H. Tweeddale, L. Notley-McRobb, T. Ferenci, J. Bacteriol. 180 (1998) 5109.
[12] R.P. Maharjan, T. Ferenci, Anal. Biochem. 313 (2003) 145.
[13] C. Wittmann, J.O. Krömer, P. Kiefer, T. Binz, E. Heinzle, Anal. Biochem. 327 (2004) 135.
[14] H. Tang, Y. Wang, J.K. Nicholson, J.C. Lindon, Anal. Biochem. 325 (2004) 260.
[15] L.M. Raamsdonk, B. Teusink, D. Broadhurst, N. Zhang, A. Hayes, M.C. Walsh, J.A. Berden, K.M. Brindle, D.B. Kell, J.J. Rowland, H.V. Westerhoff, K. van Dam, S.G. Oliver, Nat. Biotechnol. 19 (2001) 45.
[16] F. Mesnard, R.G. Ratcliffe, Photosynth. Res. 83 (2005) 163.
[17] S. Sato, T. Soga, T. Nishioka, M. Tomita, Plant J. 40 (2004) 151.
[18] W. Wang, H. Zhou, H. Lin, S. Roy, T.A. Shaler, L.R. Hill, S. Norton, P. Kumar, M. Anderle, C.H. Becker, Anal. Chem. 75 (2003) 4818.
[19] A. Lafaye, J. Labarre, J.C. Tabet, E. Ezan, C. Junot, Anal. Chem. 77 (2005) 2026.
[20] L. Wu, M.R. Mashego, J.C. van Dam, A.M. Proell, J.L. Vinke, C. Ras, W.A. van Winden, W.M. van Gulik, J.J. Heijnen, Anal. Biochem. 336 (2005) 164.
[21] M.R. Mashego, M.L.A. Jansen, J.L. Vinke, W.M. van Gulik, J.J. Heijnen, FEMS Yeast Res. 5 (2005) 419.
[22] O. Fiehn, J. Kopka, P. Dormann, T. Altmann, R.N. Trethewey, L. Willmitzer, Nat. Biotechnol. 18 (2000) 1157.
[23] M.R. Mashego, L. Wu, J.C. Van Dam, C. Ras, J.L. Vinke, W.A. Van Winden, W.M. Van Gulik, J.J. Heijnen, Biotech. Bioeng. 85 (2004) 620.
[24] G. Hopfgartner, E. Varesio, V. Tschappat, C. Grivet, E. Bourgogne, L.A. Leuthold, J. Mass Spectrom. 39 (2004) 845.
[25] W. Lu, E. Kimball, J.D. Rabinowitz, J. Am. Soc. Mass Spectrom. 17 (2006) 37.
[26] D. Gutnick, J.M. Calvo, T. Klopotowski, B.N. Ames, J. Bacteriol. 100 (1969) 215.
[27] P. Gyaneshwar, O. Paliy, J. McAuliffe, D.L. Popham, M.I. Jordan, S.J. Kustu, Bacteriology 187 (2005) 1074.
[28] C.R. Silva, I.C. Jardim, C. Airoldi, J. Chromatogr. A 987 (2003) 139.
[29] J. Xing, A. Apedo, A. Tymiak, N. Zhao, Rapid Commun. Mass Spectrom. 18 (2004) 1599.
[30] B.A. Olsen, J. Chromatogr. A 913 (2001) 113.
[31] W. de Koning, K. Van Dam, Anal. Biochem. 204 (1992) 118.
[32] S.G. Villas-Bôas, S. Mas, M. Akesson, J. Smedsgaard, J. Nielsen, Mass Spectrom. Rev. 24 (2005) 613.
[33] W.B. Dunn, N.J.C. Bailey, H.E. Johnson, Analyst 130 (2005) 606.
[34] J.I. Castrillo, A. Hayes, S. Mohammed, S.J. Gaskell, S.G. Oliver, Phytochemistry 62 (2003) 929.
[35] V.V. Tolstikov, A. Lommen, K. Nakanishi, N. Tanaka, O. Fiehn, Anal. Chem. 75 (2003) 6737.
[36] T. Soga, Y. Ohashi, Y. Ueno, H. Naraoka, M. Tomita, T. Nishioka, J. Proteome Res. 2 (2003) 488.
[37] L.C. Garratt, C.A. Ortori, G.A. Tucker, F. Sablitzky, M.J. Bennett, D.A. Barrett, Rapid Commun. Mass Spectrom. 19 (2005) 2390.
[38] Y. Guo, S. Gaiki, J. Chromatogr. A 1074 (2005) 71.
[39] V.V. Tolstikov, O. Fiehn, Anal. Biochem. 301 (2002) 298.
[40] M.R. Mashego, W.M. van Gulik, J.L. Vinke, J.J. Heijnen, Biotechnol. Bioeng. 83 (2003) 395.
[41] H.C. Lange, M. Eman, G. van Zuijlen, D. Visser, J.C. van Dam, J. Frank, M.J. de Mattos, J.J. Heijnen, Biotechnol. Bioeng. 75 (2001) 406.
[42] S.G. Villas-Bôas, J. Højer-Pederson, M. Akesson, J. Smedsgaard, J. Nielsen, Yeast 22 (2005) 1155.
[43] A.J. Wolfe, Microbiol. Mol. Biol. Rev. 69 (2005) 12.
[44] L.U. Magnusson, A. Farewell, T. Nyström, Trends Microbiol. 13 (2005) 236.
[45] B.S. Winkel, Annu. Rev. Plant Biol. 55 (2004) 85.
[46] J. Ovadi, V. Saks, Mol. Cell. Biochem. 256–257 (2004) 5.
[47] J.C. van Dam, M.R. Eman, J. Frank, H.C. Lange, G.W.K. van Dedem, S.J. Heijnen, Anal. Chim. Acta 460 (2002) 209.
[48] P. Kiefer, E. Heinzle, O. Zelder, C. Wittmann, Appl. Environ. Microbiol. 70 (2004) 229.
[49] A. Barsch, T. Patschkowski, K. Niehaus, Funct. Integr. Genomics 4 (2004) 219.
[50] E. Gstrein-Reider, M. Schweiger, EMBO J. 1 (1982) 333.